

# Enlarging the bandwidth of nanoscale propagating plasmonic modes in deep-subwavelength cylindrical holes

Peter B. Catrysse<sup>a)</sup> and Shanhui Fan

Edward L. Ginzton Laboratory and Department of Electrical Engineering, Stanford University, Stanford, California 94305-4088, USA

(Received 30 May 2007; accepted 9 October 2007; published online 1 November 2007)

Subwavelength cylindrical holes in optically thick metallic films always support a propagating  $HE_{11}$  mode near the surface plasmon frequency, regardless of how small the holes are. For holes filled with a uniform dielectric material, the bandwidth of the  $HE_{11}$  mode asymptotically approaches zero as the hole size is reduced to deep-subwavelength scales. We show that it is possible to create nanoscale propagating plasmonic modes with a very large bandwidth in holes that are concentrically filled with two different dielectric materials, *even when the hole radius goes to zero*. © 2007 American Institute of Physics. [DOI: 10.1063/1.2803849]

The optical properties of nanoapertures in optically thick metallic films have been intensely researched in the past several years due to their fundamental importance in near-field optics, and their practical significance for photonic devices and applications, including near-field probes, optical data storage, and nanolithography.<sup>1,2</sup> It is well known that the transmission characteristics are strongly influenced by the presence or absence of propagating modes inside the apertures.<sup>3,4</sup> Cylindrical holes with a circular cross section in a perfect metal do not support propagating modes when the hole diameter is smaller than  $\lambda/2n_0$ , where  $\lambda$  is the vacuum wavelength of incident light and  $n_0$  is the refractive index of the dielectric inside the hole.<sup>5</sup> Subwavelength holes in a plasmonic metal, on the other hand, always support a propagating plasmonic  $HE_{11}$  mode near the surface plasmon frequency, regardless of how small the holes are.<sup>6,7</sup> The bandwidth of this propagating mode, however, asymptotically approaches zero as the hole size is reduced to zero. Thus, such a mode may not play a prominent role as the hole size becomes far smaller than the wavelength of the incident light.

In this letter, we present a method for enlarging the bandwidth of propagating plasmonic modes in deep-subwavelength cylindrical holes by concentrically filling the holes with two different dielectric materials. We confirm the approach by dispersion analysis and three-dimensional (3D) finite-difference time-domain (FDTD) simulations. Finally, we show that by applying this method, it is possible to create nanoscale propagating modes with a very large bandwidth, *even when the hole radius goes to zero*.

The starting point for our analysis is a cylindrical hole having a circular cross-section with a radius  $r_m$  inside a metal [see inset (i) in Fig. 1]. In the hole, we define two concentric regions: a central disk with radius  $r_1$  and dielectric constant  $\epsilon_1$  and a concentric ring of width  $r_m - r_1$  and dielectric constant  $\epsilon_2$ . Both  $\epsilon_1$  and  $\epsilon_2$  are real valued and frequency independent. For the surrounding metal, we use a complex frequency-dependent plasmonic model

$$\epsilon_m(\omega) = 1 - \frac{\omega_p^2}{\omega(\omega - i\omega_\tau)}, \quad (1)$$

where  $\omega_p$  is the plasma frequency and  $\omega_\tau$  is the collision frequency. This model takes into account the contribution of free electrons only. Despite its apparent simplicity, the plasmonic model has been the source of valuable insights into the behavior of real metals. We obtain the dispersion relation  $(\beta, \omega)$  for propagating modes inside a cylindrical hole, where  $\beta$  is the real part of the complex propagation vector along the  $z$  axis of the waveguide and  $\omega$  is the radial frequency,<sup>6,7</sup> by using a transfer matrix method.<sup>8,9</sup> In what follows, we assume that  $\epsilon_m(\omega)$  takes on the form of Eq. (1) with parameter values  $\omega_p = 1.37 \times 10^{16}$  rad/s and  $\omega_\tau = 7.29 \times 10^{13}$  rad/s.<sup>7</sup> These values are representative for noble metals (in particular, silver) in the visible and near-infrared wavelength range. In addition and without the loss of generality, we set  $\epsilon_1 = 7$  (e.g., SiC) and  $\epsilon_2 = 2.13$  (e.g., SiO<sub>2</sub>). The dispersion relation for such a hole is shown as the solid red line in Fig. 1 for  $r_m = 0.36\lambda_p$  ( $\lambda_p = 2\pi c/\omega_p$ ). Specifically, the hole supports a

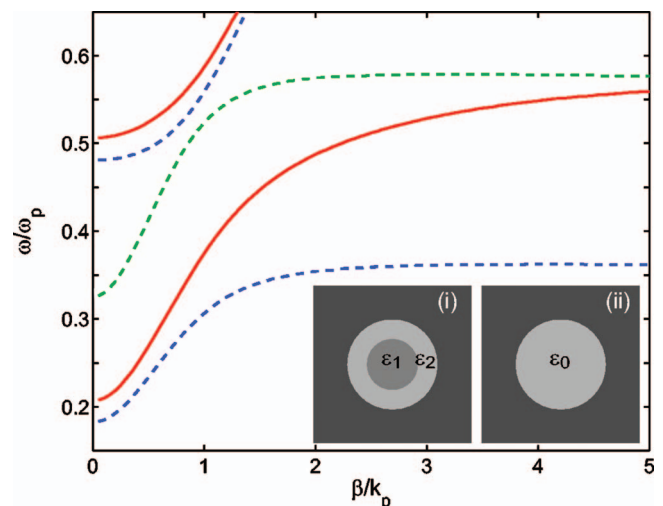


FIG. 1. (Color) Propagating plasmonic modes inside a subwavelength cylindrical hole in a metal with plasma wavelength  $\lambda_p$ . Dispersion relation for the case of a concentric high-low-dielectric core (solid red line:  $r_1 = 0.32\lambda_p$ ,  $\epsilon_1 = 7$ ,  $r_m = 0.36\lambda_p$ , and  $\epsilon_2 = 2.13$ ), a uniform low-dielectric core (dashed green line:  $r_m = 0.36\lambda_p$  and  $\epsilon_0 = 2.13$ ), and a uniform high-dielectric core (dashed blue line:  $r_m = 0.36\lambda_p$  and  $\epsilon_0 = 7$ ). Insets show the geometry.

<sup>a)</sup>Electronic mail: pcatrys@stanford.edu

lowest order  $HE_{11}$  mode extending from  $0.21\omega_p$  to  $0.57\omega_p$ , in spite of its subwavelength size (as well as a higher order  $EH_{11}$  mode). Hence, subwavelength holes using this design can, in fact, support propagating modes with a very large bandwidth.

The design principles for the concentric structure can be illustrated by considering the dispersion relation of subwavelength holes in a plasmonic metal ( $r_m=0.36\lambda_p$ ) filled with a single dielectric material  $\epsilon_0$  [see inset (ii) in Fig. 1]. The dashed blue and green curves in Fig. 1 depict the dispersion relation for propagating modes in subwavelength holes filled with a uniform dielectric, assuming  $\epsilon_0=7$  and  $\epsilon_0=2.13$ , respectively. In general, a subwavelength hole in a plasmonic metal always supports a fundamental propagating plasmonic  $HE_{11}$  mode. The upper frequency limit of the mode asymptotically approaches the surface plasmon frequency  $\omega_{sp}=\omega_p/\sqrt{\epsilon_0+1}$  of the metal-dielectric interface inside the hole when  $\beta\rightarrow\infty$ . With our choice of dielectrics, the surface plasmon frequencies are located at  $0.35\omega_p$  and  $0.57\omega_p$ , respectively. The lower frequency limit occurs for  $\beta=0$  and represents the cutoff frequency  $\omega_c$  of the  $HE_{11}$  mode. The cutoff frequency  $\omega_c$  depends on the hole radius  $r_m$ , the dielectric constant of the metal surrounding the hole  $\epsilon_m$ , and the dielectric constant of the dielectric inside the hole  $\epsilon_0$ . For the parameter values used here, the cutoff frequencies are  $0.18\omega_p$  and  $0.32\omega_p$ . We note that the limiting frequencies  $\omega_{sp}$  and  $\omega_c$  are intrinsically coupled for holes filled with a uniform dielectric. Thus, a change in the dielectric constant inside the hole leads to a shift in the frequency of the  $HE_{11}$  band without significantly affecting the bandwidth (Fig. 1, dashed green and blue curves). Moreover, the cutoff frequency  $\omega_c$  asymptotically approaches  $\omega_{sp}$  and the bandwidth of the mode,  $\omega_{sp}-\omega_c$ , asymptotically goes to zero when the hole size is reduced to zero. While subwavelength cylindrical holes with a uniform dielectric core always support a propagating mode near the surface plasmon frequency, regardless of how small the holes are, the bandwidth of the  $HE_{11}$  mode is severely reduced as the hole size shrinks to deep-subwavelength scales.

The two frequency limits  $\omega_{sp}$  and  $\omega_c$ , however, depend on the dielectric distribution inside the hole in a different fashion. For  $\beta\rightarrow\infty$ , the mode is tightly confined to the metal-dielectric interface. Hence,  $\omega_{sp}$  depends on the dielectric properties in the immediate vicinity of the interface only. At  $\beta=0$ , the mode is distributed over the entire hole and  $\omega_c$  depends on the average dielectric properties across the entire hole. The use of a concentric structure, with a high-dielectric core surrounded by a low-dielectric ring, therefore, allows one to change the average dielectric constant inside the hole without affecting the dielectric properties in the vicinity of the interface. This insight provides a mechanism for greatly enlarging the bandwidth of a subwavelength hole. As a validation of this argument, we note that the concentric structure (solid red curve in Fig. 1) has a lower cutoff frequency of  $0.21\omega_p$ , which is identical to the cutoff frequency of a hole with a uniform dielectric constant  $\epsilon_{av}=5.58$ , as determined by an appropriate dielectric average for the mode profile. The upper frequency limit of the mode asymptotically goes to  $0.57\omega_p$  and joins the large- $\beta$  frequency of the hole filled with a uniform dielectric  $\epsilon_2=2.13$ .

Figure 2 shows a vector plot of the electric displacement field for the fundamental  $HE_{11}$  mode in a subwavelength hole filled with two concentric dielectric regions. The field

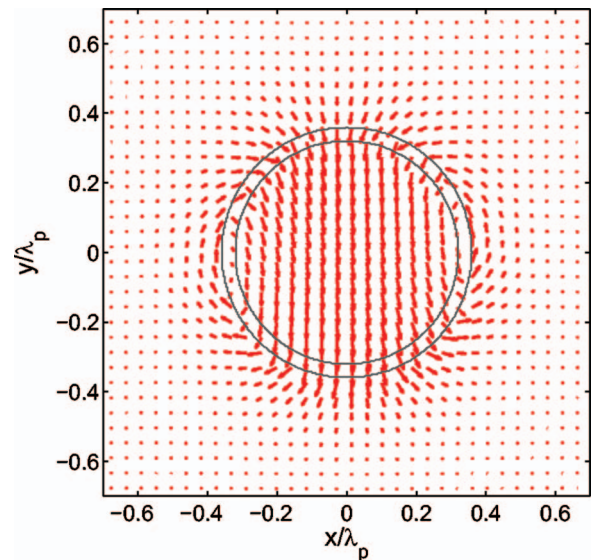


FIG. 2. (Color) Vector plots for the electric displacement field of the lowest order  $HE_{11}$  mode inside a subwavelength cylindrical hole with concentric high-low-dielectric core ( $r_1=0.32\lambda_p$ ,  $\epsilon_1=7$ ,  $r_m=0.36\lambda_p$ , and  $\epsilon_2=2.13$ ) at  $\omega=0.35\omega_p$  and  $\beta=0.85k_p$ .

orientation provides evidence that the propagating mode indeed has the proper symmetry for efficient coupling to externally incident plane waves. We have examined the fields of the next-higher-order  $EH_{11}$  mode (not shown) and confirmed that it couples to normally incident light as well.

The presence of a nonzero collision frequency leads to losses in the metal. We calculate the decay length,  $L_d=1/2\alpha$ , using the complex wave vector of the mode  $\gamma=\beta+i\alpha$ . For subwavelength holes in a plasmonic metal ( $r_m=0.36\lambda_p$ ) filled with a single dielectric material with  $\epsilon_0=7$  and  $\epsilon_0=2.13$ , the decay lengths are 1–2 and 2–3  $\mu\text{m}$  over the respective bandwidths. In the case of a concentric structure, with a high-dielectric core surrounded by a low-dielectric ring, the decay length is approximately 1–3  $\mu\text{m}$  for the extended bandwidth. Over such extended bandwidth  $\beta\gg\alpha$  (by more than an order of magnitude), the modes are clearly underdamped and hence propagating. Subwavelength holes using this design can, therefore, support propagating modes with very large bandwidth without sacrificing decay length.

Next, we consider the transmission properties of a subwavelength hole array in a metallic film of finite thickness. Figure 3 shows the spectral transmittance at normal incidence for the three cases discussed in the dispersion analysis above. The spectra are calculated using a 3D FDTD method<sup>10</sup> in which the metal is modeled as a lossy plasmonic material.<sup>7</sup> The periodicity of the array is 180 nm, the radius of the holes is  $r_m=0.36\lambda_p=50$  nm ( $\lambda_p=138$  nm), and the film thickness is  $h=250$  nm. The locations of the cutoff and limiting wavelengths agree very well with the dispersion relation of the single hole for all three cases (Fig. 1). The dashed blue and green curves depict the transmission spectrum for holes filled with a uniform dielectric material with  $\epsilon_0=7$  and  $\epsilon_0=2.13$ , respectively. Both the location of the  $HE_{11}$  pass band and the stop band between the  $HE_{11}$  and  $EH_{11}$  modes (dashed blue curve between  $0.35\lambda_p$  and  $0.48\lambda_p$ ) are in excellent agreement with the dispersion analysis of a single hole. For the solid red curve, which describes the transmission behavior of the concentric structure, the entire

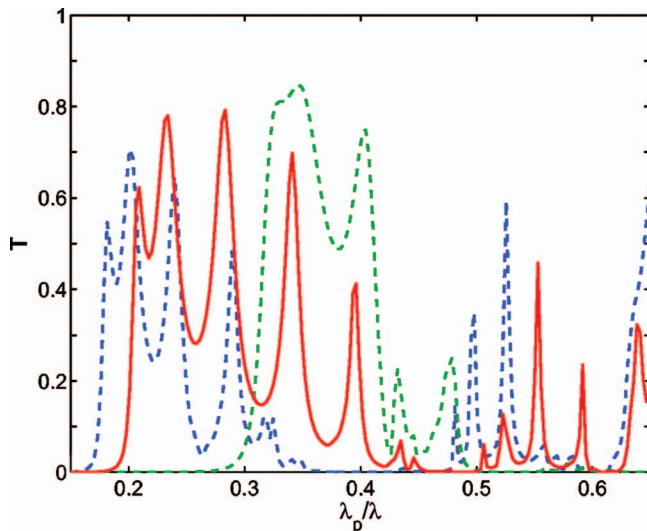


FIG. 3. (Color) Transmission at normal incidence for a square lattice of subwavelength holes in a metal film. The hole parameters are as in Fig. 1. The lattice constant is 180 nm, the radius of the holes is  $r_m=0.36\lambda_p$ ,  $r_m=50$  nm, and the film thickness is  $h=250$  nm.

range of transmission agrees well with the location of the  $HE_{11}$  and  $EH_{11}$  pass bands (Fig. 1, red curve), and their overlap results in an even larger transmission bandwidth. The dip in transmission around  $0.45\lambda_p$  is due to the band edge of the  $HE_{11}$  mode, where the mode becomes very lossy, and transmission resumes at the onset of  $EH_{11}$  mode starting at  $0.5\lambda_p$ . The bandwidth for each case can easily be determined from  $\omega_{sp}-\omega_c$ , which for the uniformly filled holes yields  $0.17\omega_p$  and  $0.25\omega_p$ , respectively. For a subwavelength hole filled with two concentric dielectric regions, on the other hand, the bandwidth is increased to  $0.36\omega_p$ . This confirms that by engineering the dispersion of a single hole according to our method, it is possible to significantly extend the transmission bandwidth for metallic systems based on subwavelength holes.

While the ability to independently design the lower and upper frequency limits of propagating modes is useful in extending the bandwidth for any size subwavelength hole, this general idea for enhancing the pass band is particularly powerful for systems based on nanoscale geometries. As an illustration, Fig. 4 shows the dispersion curves for propagating modes in the extreme case of nanoscale holes with  $r_m=0.036\lambda_p=5$  nm. The dashed blue and green curves depict the dispersion curves for  $\epsilon_1=7$  and  $\epsilon_2=2.13$ , respectively. In comparison with the 50 nm holes (bandwidths  $0.17\omega_p$  and  $0.25\omega_p$ ), the bandwidth of plasmonic modes is severely reduced (by an order of magnitude) as the hole size shrinks to deep-subwavelength scales. For the solid red curve, on the other hand, the bandwidth remains large. Despite the ten times reduction in hole size, the bandwidth is only decreased by half. While it is known that a local material model no longer reflects the metal properties at such extreme small length scales, this example nevertheless illustrates the general applicability of our approach.

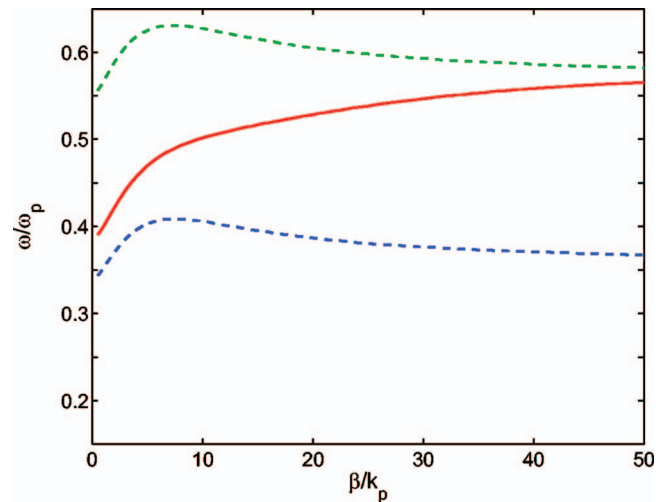


FIG. 4. (Color) Propagating  $HE_{11}$  modes inside a nanoscale cylindrical hole in a metal with plasma wavelength  $\lambda_p$ . Dispersion relation for the case of a concentric high-low-dielectric core (solid red line:  $r_1=0.032\lambda_p$ ,  $\epsilon_1=7$ ,  $r_m=0.036\lambda_p$ , and  $\epsilon_2=2.13$ ), a uniform low-dielectric core (dashed green line:  $r_m=0.036\lambda_p$  and  $\epsilon_0=2.13$ ), and a uniform high-dielectric core (dashed blue line:  $r_m=0.036\lambda_p$  and  $\epsilon_0=7$ ).

The ability to decouple the frequency limits of the plasmonic  $HE_{11}$  mode band, through multiple concentric dielectric regions, enables the design of deep-subwavelength holes that support nanoscale plasmonic modes with a very large bandwidth. As an additional benefit of this method, the spectral location of the propagating mode is no longer in the vicinity of the surface plasmon frequency; rather its cutoff frequency can be engineered to lie anywhere below the surface plasmon frequency, which allows the utilization of frequency regions where metals have lower loss. Finally, we have verified that the conclusions of this paper remain valid for more complex material models (e.g., the Lorentz-Drude model).

This work was supported in part by the Stanford Global Climate and Energy Project (GCEP), and by the NSF-NIRT Program (Grant No. ECS-0507301). The computation was performed with support from the NSF-LRAC program.

<sup>1</sup>For an overview, see the focus issue on “Extraordinary light transmission through sub-wavelength structured surfaces,” *Opt. Express* **12**, 3618 (2004).

<sup>2</sup>C. Genet and T. W. Ebbesen, *Nature (London)* **445**, 39 (2007).

<sup>3</sup>F. I. Baida and D. Van Labeke, *Phys. Rev. B* **67**, 155314 (2003).

<sup>4</sup>J. A. Porto, F. J. Garcia-Vidal, and J. B. Pendry, *Phys. Rev. Lett.* **83**, 2845 (1999).

<sup>5</sup>W. L. Barnes, A. Dereux, and T. W. Ebbesen, *Nature (London)* **424**, 824 (2003).

<sup>6</sup>L. Novotny and C. Hafner, *Phys. Rev. E* **50**, 4094 (1994).

<sup>7</sup>H. Shin, P. B. Catrysse, and S. Fan, *Phys. Rev. B* **72**, 085436 (2005).

<sup>8</sup>M. Ibanescu, Y. Fink, S. Fan, E. L. Thomas, and J. D. Joannopoulos, *Science* **289**, 415 (2000).

<sup>9</sup>P. Yeh, A. Yariv, and E. Marom, *J. Opt. Soc. Am.* **68**, 1196 (1978).

<sup>10</sup>Allen Taflov and Susan C. Hagness, *Computational Electrodynamics: The Finite-Difference Time-Domain Method*, 2nd ed. (Artech House, Boston, 2000), Chap. 3, p. 75.